Biosensors and Bioelectronics 87 (2017) 1036–1043

Contents lists available at ScienceDirect

Biosensors and Bioelectronics

journal homepage: www.elsevier.com/locate/bios

Reconstituting redox active centers of heme-containing proteins with biomineralized gold toward peroxidase mimics with strong intrinsic catalysis and electrocatalysis for H_2O_2 detection

Liyan Zhang[a], Shuai Li[a], Minmin Dong[a], Yao Jiang[a], Ru Li[a], Shuo Zhang[a], Xiaoxia Lv[a], Lijun Chen[b], Hua Wang[a,*]

[a] Shandong Province Key Laboratory of Life-Organic Analysis, College of Chemistry and Chemical Engineering, Qufu Normal University, Qufu City, Shandong 273165, P.R. China

[b] Hospital of University, Qufu Normal University, Qufu City, Shandong Province 273165, P.R. China

ARTICLE INFO

Keywords:
Enzyme reconstitution
Redox active centers
Gold biomineralization
Peroxidase mimics
Intrinsic catalysis

ABSTRACT

A facile and efficient enzymatic reconstitution methodology has been proposed for high-catalysis peroxidase mimics by remolding the redox active centers of heme-containing proteins with the in-site biomineralized gold using hemoglobin (Hb) as a model. Catalytic hemin (Hem) was extracted from the active centers of Hb for the gold biomineralization and then reconstituted into apoHb to yield the Hem-Au@apoHb nanocomposites showing dramatically improved intrinsic catalysis and electrocatalysis over natural Hb and Hem. The biomineralized gold, on the one hand, would act as "nanowires" to promote the electron transferring of the nanocomposites. On the other hand, it would create a reactivity pathway to pre-organize and accumulate more substrates towards the active sites of the peroxidase mimics. Steady-state kinetics studies indicate that Hem-Au@apoHb could present much higher substrate affinity (lower Michaelis constants) and intrinsic catalysis even than some natural peroxidases. Moreover, the application feasibility of the prepared artificial enzymes was demonstrated by colorimetric assays and direct electrocatalysis for H_2O_2 sensing, showing a detection limitation low as 0.45 μM. Importantly, such a catalysis active-center reconstitution protocol may circumvent the substantial improvement of the intrinsic catalysis and electrocatalysis of diverse heme-containing proteins or enyzmes toward the extensive applications in the chemical, enviromental, and biomedical catalysis fields.

1. Introduction

Natural enzymes such as horseradish peroxidase (HRP) and glucose oxidase (GO) have been widely applied in pharmaceutical process, chemical industry, food processing, and biosensing fields, due to they possess the high catalysis efficiencies and specificities (Clouthier and Pelletier, 2012; Wilson and Nie, 2006). In human body, there also are some heme-containing proteins, such as hemoglobin (Hb), myohemoglobin (Mb), and cytochrome c, which play a vital role in life activities by conducting various functions like oxygen transportation and peroxidase-like biochemical catalysis (McCarthy et al., 2001; Xie et al., 2012). However, the practical applications of these cost-effective catalytic proteins are mostly challenged by some disadvantages like low catalysis activities and environmental instability (Huang et al., 2011; Wang et al., 2014a, 2014b). Therefore, huge efforts have been contributed to the employment of these cheap catalytic proteins for the fabrication of enzymatic mimics with improved catalysis performances (Wang et al., 2014a, 2014b; Wei and Wang, 2013).

It has been established that the catalysis-active centers of natural enzymes and catalytic proteins are normally located deeply into their protein pockets. For example, the catalysis-active centers of heme-containing proteins (i.e., Hb) are generally embedded in their polypeptide chain structures (Heller, 1990). Accordingly, the direct improvement of the active centers of heme enzymes can be of vital importance in improving their intrinsic catalysis capacities especially electrocatalysis. As a very effective example, the enzymatic reconstitution protocol of natural enzymes and catalytic proteins have been reported for Hb (Torres et al., 2002), Mb (Hayashi et al., 1999), GO (Willner et al., 1996), HRP (Ryabov et al., 1999; Song et al., 2009), and cytochrome c (Hayashi et al., 1998), mostly by way of organic functional modifications of redox active centers to enhance the electron transferring to attain the enhanced catalysis efficiency. Nevertheless, the issues regarding the substantial improvement of the intrinsic catalytic activities of natural enzymes and low-catalysis proteins are

* Corresponding author.
E-mail addresses: huawangqfnu@126.com (H. Wang).

http://dx.doi.org/10.1016/j.bios.2016.09.075
Received 18 September 2016; Accepted 21 September 2016
Available online 22 September 2016
0956-5663/

far from being addressed due to the formidable inaccessibility of their catalysis-active sites, which may to some degree bottleneck their practical applications on a large scale in chemical and biological catalysis fields.

In recent decades, many versatile nanomaterials, most known as gold nanoparticles, have been increasingly applied for improving the catalysis properties of natural enzymes (Patolsky et al., 2004; Shamsipur et al., 2015; Wang and Astruc, 2014; Xia et al., 2009; Xiao et al., 2003; Yang et al., 2015; Yehezkeli et al., 2009). Due to some unique features such as large surface-to-volume ratio, high catalytic efficiency, and strong adsorption ability, gold nanoparticles (AuNPs) have been widely utilized to label or anchor enzymes (i.e., HRP) so as to accelerate the electron transferring toward the improved electrocatalysis (Patolsky et al., 2004; Shamsipur et al., 2015; Xia et al., 2009; Xiao et al., 2003; Yehezkeli et al., 2009). For example, Tian's group has immobilized Mb on nanopyramidal gold surfaces to realize the determination of H_2O_2 at low redox potency (i.e., 0.21 V) without a mediator (Xia et al., 2009). Willner et al. employed small AuNPs to electrically contact the redox-active centers of the reconstituted enzyme (i.e., GO) on the electrode supports to develop a highly efficient electrocatalysis system (Patolsky et al., 2004; Xiao et al., 2003). More recently, Mojtaba and co-workers have directly capped nanoclusters with Hb for the highly sensitive electroanalysis of hydrogen peroxide (Shamsipur et al., 2015). These pioneering works have achieved the great enhancement of the electrocatalysis performances of varying heme-containing enzymes typically by using gold nanomaterials. However, the improvement of the intrinsic catalysis activities of these redox enzymes has remained far from being solved to date, presumably due to that these extraneously-synthesized nanomaterials might largely be anchored outside the redox "active sites" of native enzymes (Xiao et al., 2003). Moreover, it has been widely recognized that the redox substrates in the enzyme-catalyzed reactions should be ideally pre-organized at the pockets close to the active sites of enzymes so as to facilitate the highly efficient transformations (Dydio and Reek, 2014; Raynal et al., 2014a, 2014b; Wang et al., 2016). For example, Reek et al. proposed a novel catalysis design for the substrate pre-organization by encapsulating the catalysts and substrates within the confined space defined by the self-assembled nanospheres for highly efficient catalytic reactions (Wang et al., 2016). It is thereby inspired that creating a reactivity pathway of high substrate affinity for the pre-organization of substrates toward the catalysis active sites of heme enzymes can be considered as another crucial way of improving the catalysis performances of heme-containing enzymes and proteins.

In the present work, we have developed a novel enzymatic reconstitution methodology for remolding the redox active centers of heme-containing enzymes or proteins with the gold "nanowires" by the in-site biomineralization way toward the high-catalysis peroxidase mimics using Hb as a model. It has been well recognized that Hb is a heme-containing protein with peroxidase-like catalysis and well-known structure (Heller, 1990) can be suffered from the considerably low catalysis activity for the practical applications. In a previous work, we have developed a protein-based biomineralization route to successfully improve the hydrolytic catalysis of alkaline phosphatase (Si et al., 2014). When such a route was applied to remold Hb and some peroxidases (i.e., HRP), however, no significant enhancement of intrinsic catalysis activities was achieved for these catalytic proteins and enzymes except for the electrocatalysis, presumably due to that their catalysis-active sites (i.e., heme) should be buried so deeply in the specific proteomic microenvironments that it may be hard to be accessed (Andersen et al., 2012; Jones et al., 2012; Mai et al., 2010). Alternatively, herein, the redox active center was extracted from Hb to produce catalytic hemin (Hem) and apoHb. Thereafter, Hem was remolded with biomineralized gold (Hem-Au) by the biomineralization way (Si et al., 2014; Xie et al., 2009) and then reconstituted into apoHb to yield the Hem-Au@apoHb nanocomposite (Scheme 1). Herein, the biomineralized gold could act as "nanowire" to promote the electron-transferring of redox active site of Hem in Hem-Au@apoHb nanocomposites. Meantime, it would substantially cause the conformational change of the Hem-Au@apoHb nanocomposite to construct the reactivity pathways for pre-organizing more substrates to their redox active sites. The so developed peroxidase mimics would be expected to circumvent the improved intrinsic catalysis and electrocatalysis activities in catalyzing the typical redox reactions of 3, 3′, 5, 5′-tetramethyl benzidine (TMB) and H_2O_2. Systemic characterizations were conducted for the as-prepared Hem-Au@apoHb nanocomposites. Moreover, the catalysis performances of Hem-Au@apoHb nanocomposites were investigated in comparison to native Hb and Hem. Moreover, steady-state kinetics studies were conducted for the developed peroxidase mimic in terms of the substrate affinity and intrinsic catalysis capacities in comparison to native Hb and some peroxidases like HRP. Additionally, the direct electroanalysis of the as-developed nanocomposites for H_2O_2 was confirmed. To the best of our knowledge, this is the first success on the substantial enhancement of the intrinsic catalysis and electrocatalysis activities of heme-containing enzymes or proteins through the remolding and reconstitution of gold "nanowired" redox active centers by the in-site biomineralization way.

2. Experimental

2.1. Reagents and apparatus

Hemoglobin (Hb, MW 66000) and Hemin (Hem) from bovine

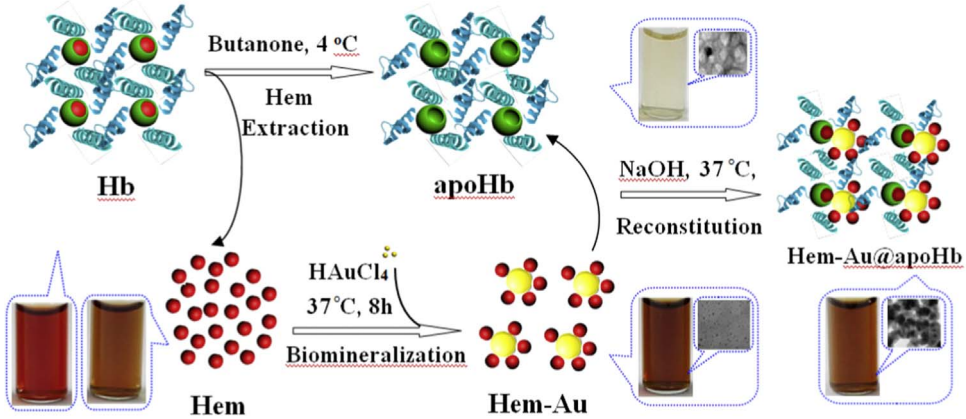

Scheme 1. Schematic illustration of the reconstitution-based synthesis procedure of Hem-Au@apoHb nanocomposite, including the Hem extraction and apoHb preparation, the gold biomineralization with AuNPs to form Hem-Au core, and the reconstitution of Hem-Au into apoHb through its attached Hem molecules, with the photographs of corresponding product solutions of Hem-Au and Hem-Au@apoHb nanocomposites.

blood were purchased from Sigma to be used without further purification. Hydrogen tetrachloroaurate ($HAuCl_4$), citric acid, methylethylketone, and phosphate buffer solution (PBS, pH 7.4) were obtained from Aladdin Reagent Co., Ltd. (Shanghai, China). 3,3′,5,5′- tetramethyl benzidine (TMB), TMB- H_2O_2 chromogenic substrate, and chitosan were purchased from Sinopharm Chemical Reagent Co. (China). All other reagents are of analytical grade. Deionized water (> 18 MΩ) was supplied from an Ultrapure water system (Pall, USA).

The colorimetric measurements of the catalytic activities of enzymes and mimics were performed by a microplate reader (Infinite M200 PRO, Tecan, Austria) and 96-well plates (JET BIOFIL, Guangzhou, China). Transmission electron microscopy (TEM, FEI Tecnai G20, USA) imaging operated at 100 kV and energy dispersive spectroscopy (EDS) were employed to characterize the nanomaterials and composites. Uv–vis absorption spectra were collected using UV-3600 spectrophotometer (Shimadzu, Japan) equipped with a thermostated holder, and fourier transform infrared (FTIR) spectra were obtained by FTIR spectrophotometer (Thermo Nicolet Nexus 470FT, USA). Elemental mapping measurement was conducted using a scanning electron microscope (SEM, Hitachi E-1010, Horiba Ex-250) with microanalysis system (EDAX, USA). The percents of Fe and Au elements in different samples were analyzed with an inductively coupled plasma mass spectrometer (ICP-MS) of Agilent 7500ce (Agilent Technologies, Waldbronn, Germany). Thermostatic mixing was performed by DF101 collector-type temperature magnetic stirrer (Gongyi Corey Ltd.). Moreover, the electrochemical measurements were carried out using the electrochemical workstation CHI 760D (CH Instruments, Shanghai, China) connected to a personal computer. Additionally, the electrochemical three-electrode system was used consisting of the modified glassy carbon (GC) electrode as the working electrode, a platinum wire as a counter electrode and an Ag/AgCl electrode as the reference electrode.

2.2. Extraction of heme from Hb yielding Hem and apoHb

Hemin (Hem) and apoHb were obtained by extracting heme from Hb according to a modified synthesis procedure reported elsewhere (Song et al., 2009). Briefly, an aliquot of Hb (0.26 g) was dissolved in 2.0 mL ice-cold water in the ice-bath. Under vigorous stirring, $K_3Fe(CN)_6$ (10 mg mL^{-1}) was dropped into the Hb solution to proceed for 20 min to oxidize heme to Hem there. Then, the mixture was dialyzed in PBS (pH 7.4) for 2 h, followed by the adjustment of pH value to about 2.0. Moreover, an aliquot of ice-cold methylethylketone was introduced into the mixture to extract the Hem in the supematant liquor under vigorous stirring. The yielded supematant liquor containing Hem was separated in base solution and collected to be stored at 0 °C. Further, the apoHb-containing underlayer liquor was dialyzed separately against $NaHCO_3$ (5.0 mM), water, and PBS (pH 7.4) to remove any methylethylketone and other low-molecular-weight impurities. Subsequently, the as-prepared apoHb products were collected by centrifuge to be stored at 4 °C for future usage.

2.3. Synthesis of Hem-Au cores

Under vigorous stirring, $HAuCl_4$ (1.0 mL, 10 mM) was mixed with Hem solution (1.0 mL, 0.80 mg mL^{-1}), followed by the addition of an aliquot of NaOH (120 μL, 1.0 M). After the mixture was stirred for 8 h at 37 °C, the Hem with biomineralized gold (Hem-Au) was dialyzed in water for 8 h using the membrane (pore size of 1.8 nm or molecular weight of 20 KD), of which the cut-off particle size or molecular weight was close to that of Hem-Au_{25} (Xie et al., 2009). Finally, the so prepared Hem-Au cores were stored at 4 °C for future usage.

2.4. Reconstitution of Hem-Au cores into apoHb shells

The reconstitution procedure of Hem-Au cores into apoHb shells was carried out as follows. Under vigorous stirring, the Hem-Au cores were mixed with apoHb shells at the optimized molar ratio (Hem-Au:apoHb=5: 1), followed by the adjustment of pH value to about 9.0–10.0 by using 0.10 M NaOH. After the reconstitution proceeded for 8 h at 37 °C, the resulting Hem-Au@apoHb nanocomposites were separated by centrifuge to remove the byproducts. Subsequently, a purification procedure was further applied with Sephadex G-75 column and membrane (pore size of 5.5 nm or molecular weight of 100 KD), of which the cut-off molecule weight was close to that of intact Hb. The so obtained Hem-Au@apoHb products were collected to be stored at 4 °C for future usage.

2.5. Colorimetric assays

The colorimetric assays for the comparable investigation of peroxidase-like activities were conducted by using the TMB-H_2O_2 chromogenic reactions. Typically, an aliquot of the prepared nanocomposites was introduced into the TMB-H_2O_2 reactions, of which the reaction products were monitored by UV–visible absorbance at 652 nm using 96-well plates and a microplate reader. Accordingly, the comparison of enzymatic catalysis activities was carried out by the colorimetric assays for native Hb, Hem, Hem-Au, and apoHb as the controls. Moreover, the optimization of the main conditions for the synthesis of Hem-Au cores were performed using different NaOH amounts (0.020–0.20 M), Hem dosages (0.10–5 mg mL^{-1}), and reaction time. Also, the core-shell ratios-dependent catalysis activities of Hem-Au@apoHb were carried out at the different molar ratios of Hem-Au to apoHb, so did the catalytic conditions for the TMB-H_2O_2 reactions at different pH values 2.0–12) and temperature (20–55 °C). Additionally, steady state kinetic studies were comparably carried out for Hem-Au@apoHb and Hb (each containing 4.06 μM Hem), where 1.60 mM H_2O_2 or 0.62 mM TMB was used alternatively at a fixed concentration of one substrate versus varying concentration of the second substrate. The Lineweaver-Burk plots by the double reciprocal of the Michaelis–Menten equation were thus performed to calculate the Michaelis-Menten constants.

Of note, the Hem levels in the tested Hem-containing materials like Hem-Au@apoHb nanocomposites and Hb were determined from the results of the UV–vis absorbance measurements by referring to the plotted standard Hem concentration-absorbance curve.

2.6. Electrochemical measurements

An aliquot of Hem-Au@apoHb was first mixed with 2.0 mg mL^{-1} chitosan dissolved in 2.0% acetic acid. Then, 3.0 μL of the above mixture was casted onto the surface of the pretreated GC electrodes, which were regenerated after usage by polishing procedures, and then dried at room temperature overnight to form the Hem-Au@apoHb modified electrodes. In a typical electrochemical experiment, cyclic voltammetry (CV) and linear sweep voltammetry (LSV) were separately performed for the resulting electrodes in PBS over the potential range of −0.60–0.50 V at a scanning speed of 50 mV/s. Moreover, the comparison of electrocatalysis was performed between the Hem-Au@apoHb electrodes and the electrodes modified with native Hb that were prepared according to the same procedure. In addition, the electrocatalysis properties of the Hem-Au@apoHb electrodes towards different H_2O_2 concentrations were explored, with the current responses recorded for different concentrations of H_2O_2 ranging from 0.0018 to 2.50 mM. A baseline correction of the resulting voltammograms was performed with the CHI software.

3. Results and discussion

3.1. Synthesis and characterization of peroxidase mimic of Hem-Au@apoHb

It has been widely recognized that a Hb molecule possesses the

redox-active center of four heme molecules that are inaccessibly embedded into the polypeptide chain structures, showing a low peroxidase-like catalysis activities in various H_2O_2 biosensors (Chen et al., 2012; Shan et al., 2007). Initially, we directly encapsulated gold nanoclusters with intact Hb by using the protein-based gold biomineralization route reported elsewhere (Si et al., 2014; Xie et al., 2009; Zhang et al., 2014). However, no significant improvement of intrinsic catalysis activities was realized for Hb, presumably due to that the yielded gold "nanowires" might only anchor outside Hb molecules, of which the redox active sites of heme might remain untouched. In the present work, a novel reconstitution methodology has been developed for Hb alternatively by extracting the catalytic active centers from Hb to produce Hem for the in-site gold biomineralization, followed by the reconstitution into apoHb. The main synthesis and reconstitution protocol is schematically illustrated in Scheme 1, in which Hem was drawn schematically as a "ball" to show how it was shaped on AuNP by the in-site biomineralization way and further reconstituted into the pocket of apoHb. Under the acidic conditions, a slightly conformational denaturation of Hb protein might occur so as to weaken the interactions involved such as hydrogen bond and salt bridges (Boys et al., 2007), leading to the quick release of heme from Hb to yield Hem and apoHb. Furthermore, small Au ions could be introduced to react with the functional groups of Hem scaffolds like pyrroles to conduct the in-site gold biomineralization, where Hem could serve as the stabilizer and reducing agents. The resulting Hem-Au was subsequently reconstituted into apoHb through its attached Hem molecules to yield the Hem-Au@apoHb nanocomposite, of which Hem-Au might partly stick out of the protein shell of apoHb as illustrated in Scheme 1. Such a gold-wired reconstitution mode of Hem-Au in apoHb might practically present the synergic effects on the enhanced catalysis and electrocatalysis of the resulted nanocomposites, since the enzyme catalysis should depend mainly on the turnover rate of electron transfer of catalysis-active centers as demonstrated elsewhere (Xiao et al., 2003). That is, the so biomineralized gold would act as "nanowires" for the catalysis-active Hem to promote the electron transferring in catalyzing the redox reactions. Meantime, they would substantially trigger the conformational changes of Hem-Au@apoHb nanocomposites to create the reactivity pathways with high substrate affinity for pre-organizing more substrates toward the active sites. Therefore, the so prepared peroxidase mimics of nanocomposites could be expected to achieve the greatly improved intrinsic catalysis and electrocatalysis activities in catalyzing the redox reactions typically using H_2O_2. Yet, it is worth pointing out that the detailed reconstitution mechanism would be investigated in the future work.

The topological investigations of Hem-Au@apoHb nanocomposites were conducted by TEM imaging (Fig. 1). It was found that the obtained Hem-Au cores were highly uniform and well dispersed in water, showing an average particle size of about 2.0–3.0 nm in diameter (Fig. 1A). Herein, the extracted Hem molecules might be attached onto the bigger AuNPs that were formed in site by the Hem-mediated biomineralization way, of which the detailed formation mode will be further investigated. Particularly, the biomineralized gold at catalysis-active Hem could display the clear gold crystalline lattices to expect the functional "nanowires" for the electron shuttling of Hem, as apparently manifested in the magnitude-amplified view (Fig. 1B). Moreover, the developed Hem-Au@apoHb nanocomposites could present the ellipse structure with the average size of about 7.0 nm in diameter but most in aggregation (Fig. 1C), which is basically consistent with the protein size of Hb (Erickson, 2009) and apoHb (Fig. 1D). Fig. 1E shows the magnitude-amplified TEM image of the aggregated Hem-Au@apoHb nanocomposites, on which gold signatures were furnished throughout with apparent crystalline lattices, indicating the reconstitution of Hem-Au cores into the apoHb shells. Moreover, the conformation of Hem-Au@apoHb nanocomposites was

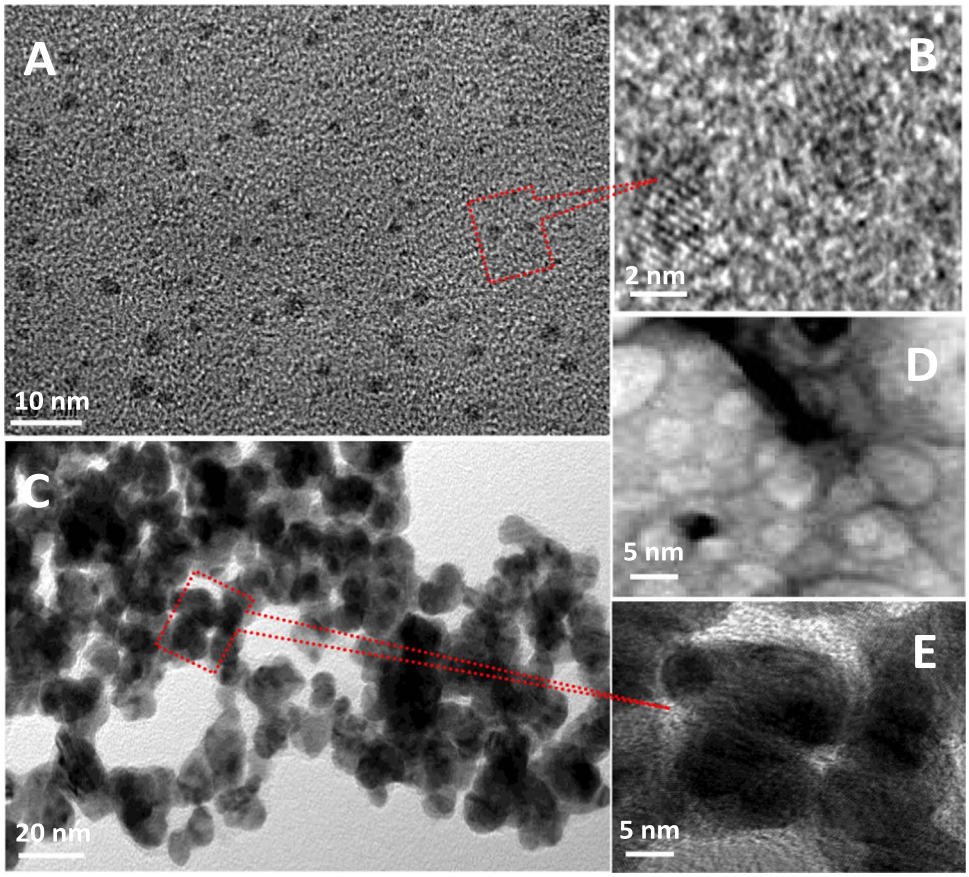

Fig. 1. TEM images of Hem-Au of (A) low and (B) high magnifications, and Hem-Au@apoHb nanocomposites of (C) low and (E) high magnifications and (D) apoHb.

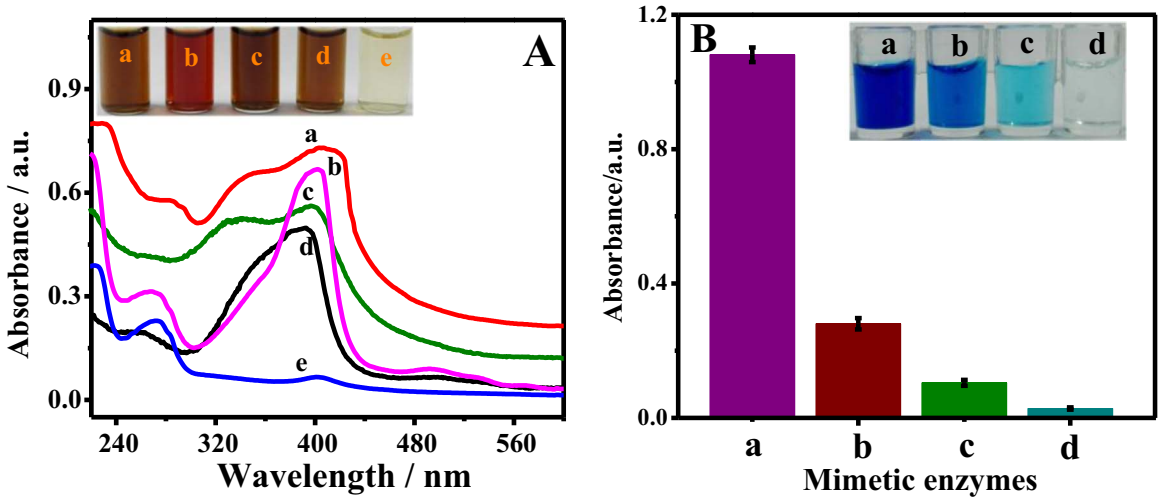

Fig. 2. (A) Comparison of UV–vis spectra among (a) Hem-Au@apoHb, (b) Hb, (c) Hem-Au, (d) Hem, and (e) apoHb. (B) Comparison of catalysis activities among (a) Hem-Au@apoHb, (b) Hb, (c) Hem, and (d) apoHb in catalysing the TMB-H_2O_2 reactions, of which the absorbances of the products were recorded for the mimetic enzymes containing 4.06 μM Hem if any, with the corresponding photographs (insert).

studied by the UV–vis spectra, taking Hb, Hem-Au, Hem, and apoHb as the controls (Fig. 2A). It was discovered that native Hb (curve b) could present the heme and protein absorbance peaks at about 405 nm and about 280 nm, respectively. After heme was extracted from Hb, the two peaks could be separated to appear exclusively in corresponding Hem (curve d) and apoHb (curve e). Moreover, when Hem was remolded with the biomineralized gold to form the Hem-Au (curve c), both of the absorbance peaks of Hem (405 nm) and biomineralized gold (330 nm) could be witnessed, thereby confirming the formation of Hem-Au. More importantly, the Hem-Au@apoHb nanocomposites (curve a) could include three kinds of characteristic absorbance peaks of Hem, biomineralized gold, and apoHb protein, which could mostly show a little shift compared to those of the mixture consisting of Hem, AuNPs, and apoHb (i.e., the absorbance peak of Hem) as disclosed in Fig. S1, indicating the successful reconstitution of Hem-Au into apoHb. Fig. S2 shows a comparison of FTIR spectra between Hb (red) and Hem-Au@apoHb (black). It was found that the peak of Hb at about 1533 cm^{-1} disappeared for Hem-Au@apoHb (black). Instead, two rather sharp bands emerged separately peaking at about 1150 cm^{-1} and 1200 cm^{-1}. The results indicated that AuNPs in Hem-Au@apoHb might induce a conformational change of the secondary structure of Hb protein (Shamsipur et al., 2015). Moreover, the elemental analysis with EDS was performed for Hem-Au@apoHb (Fig. S3), showing the presence of Au and Fe elements. Also, from the SEM imaging with elemental mapping for Hem-Au@apoHb, one can note that Fe and Au elements were uniformly dispersed in the nanocomposites in a discretely mixed way (Fig. S4), showing a spatially resolved distribution of Hem-Au@apoHb. Furthermore, a percentage comparison of Fe and Au elements was conducted among Hem, Hem-Au, Hb, and Hem-Au@apoHb by using the ICP-MS, with the data summarized in Table S1. It was discovered that Hem and Hem-Au possessed the appropriate Fe contents, so did Hb and Hem-Au@apoHb, which might prove the well-retained Fe elements in these testing samples. The above results demonstrate that Hem-Au was successfully reconstituted into apoHb to yield Hem-Au@apoHb nanocomposite.

3.2. Colorimetric investigations of Hem-Au@apoHb nanocomposites

The catalysis properties of Hem-Au@apoHb nanocomposites were investigated by the colorimetric system using the TMB- H_2O_2 reaction, in comparison to native Hb and Hem, each containing the same dosage of Hem (Fig. 2B). One can note that the catalysis activity of Hem-Au@apoHb (a) was about four- and 10-fold stronger than those natural Hb (b) and Hem (c), respectively. Notably, apoHb (d) showed no significant catalysis in the TMB-H_2O_2 reactions. As aforementioned, herein, the biomineralized gold could not only functionalize as the "nanowires" to accelerate the electron transferring of catalysis-active Hem, but also created the reactivity pathways of high substrate affinity for pre-organizing more substrates (i.e., TMB) to the redox active sites. Therefore, the Hem-Au@apoHb nanocomposite developed by the enzymatic reconstitution methodology could provide much stronger intrinsic catalysis activities than natural catalytic proteins like Hb.

3.3. Optimization of the main fabrication conditions

The main experimental conditions for the synthesis and reconstitution of Hem-Au toward the Hem-Au@apoHb nanocomposites were optimized (Fig. S5). First, NaOH could play a vital role in the preparation of catalytic Hem-Au by the protein-based gold biomineralization route. It was found that the catalysis activities of Hem-Au could increase with the increasing concentrations of NaOH till 0.060 M (Fig. S5A), over which a gradual decrease in the catalysis activities of Hem-Au could be encountered. Second, the dosage of Hem scaffolds used for the fabrication of Hem-Au was explored by using different Hem concentrations (Fig. S5B). Obviously, an aliquot of 0.40 mg mL^{-1} Hem in the gold biomineralization reaction was suitable for yielding the Hem-Au. Third, the reaction time for the gold biomineralization toward the formation of Hem-Au was investigated (Fig. S5C), showing the optimum time of 8 h. Here, too long reaction time might risk the formation of larger AuNPs leading to the worse catalysis and stability of Hem-Au. Finally, the ratios of Hem-Au core to apoHb shell were optimized for the reconstitution of Hem-Au toward the enzyme mimics (Fig. S5D). One can find that the Hem-Au to apoHb ratio of about 5:1 should be the optimum one to be selected for the formation of Hem-Au@apoHb nanocomposite. Such a molar ratio is basically consistent to the practical composition of a natural Hb molecule that consists of four Hem molecules.

3.4. Optimization of the catalytic reaction conditions

The main catalysis conditions like pH values and temperature were investigated for the Hem-Au@apoHb by using the TMB-H_2O_2 reactions. Fig. S6A displays the pH value-depending catalysis performances of Hem-Au@apoHb, taking natural Hb as a comparison. As is shown in Fig. S6A, Hem-Au@apoHb could perform the best catalysis at pH 8.0, in contrast to the optimum one of natural Hb at pH 10. The results suggest that Hem-Au@apoHb might conduct the catalysis under the slightly alkaline condition. Furthermore, the temperature-dependent

catalysis of Hem-Au@apoHb was studied with the TMB-H_2O_2 reactions (Fig. S6B). Accordingly, the developed peroxidase mimics showed the highest catalysis activities at about 37 °C, in good consistence with natural Hb. These results indicate that Hem-Au@apoHb and Hb might conduct the catalysis under the basically similar reaction conditions. Therefore, the developed enzymatic reconstitution route might well sustain the main functional structure of Hb molecules, yet, dramatically improve their intrinsic catalysis activities by the reconstitution of gold-"nanowiring" active centers forming the Hem-Au@apoHb.

3.5. Studies on steady-state catalysis kinetics

Steady-state catalysis kinetics was studied for the developed Hem-Au@apoHb by using the Michaelis–Menten model, taking natural Hb as the comparison (Fig. S7). One can observe that the plotting of initial reaction rates versus varying TMB amounts (Fig. S7A) or H_2O_2 concentrations (Fig. S7B) could illustrate the typical Michaelis–Menten behavior. Importantly, the comparison of the colorimetric results between Hem-Au@apoHb (red curve) and natural Hb (black curve) reveals that the as-prepared peroxidase mimics could display much better catalysis performances than native Hb. Moreover, the dynamic parameters including Michaelis constant (K_m), the maximal reaction velocity (V_{max}), and the catalytic constant (K_{cat}) were calculated by the regression of Lineweaver-Burk double reciprocal curves (Fig. S7), with the results summarized in Table S2 taking Hb and HRP reported elsewhere (Gao et al., 2007) as the comparisons. One can note that the apparent K_m value of Hem-Au@apoHb for H_2O_2 (2.05 mM) is much lower than that of native Hb (2.85 mM) or HRP (3.70 mM). Meanwhile, the K_m value of the developed peroxidase mimics for TMB substrate is 0.270 mM, which is also much lower than that of Hb (2.78 mM) but approximate to that of HRP (0.434 mM). Moreover, Hem-Au@apoHb could present higher V_{max} values for both substrates than native Hb and HRP (Gao et al., 2007). Particularly, the catalytic specificity constant of K_{cat}/K_m of Hem-Au@apoHb for TMB is much higher than that of Hb and close to that of HRP. However, the developed nanocomposites could display much higher K_{cat}/K_m value for H_2O_2 than Hb or HRP. These data demonstrate that Hem-Au@apoHb could exhibit considerably high substrate affinity and catalysis, presumably due to that the biomineralized gold could build up the catalytic reactivity pathways to pre-organize more substrates (i.e., H_2O_2 and TMB) towards their catalysis-active sites to facilitate the highly efficient transformations of substrates (Dydio and Reek, 2014; Raynal et al., 2014a, 2014b; Wang et al., 2016). Therefore, much stronger intrinsic catalysis and electroanalysis activities could be expected for the developed Hem-Au@apoHb, due to the catalytic reactivity pathways of high substrate affinity transferring in catalytic redox reactions. Furthermore, the environmental storage stability of the as-developed Hem-Au@apoHb was probed by monitoring their time-dependent catalysis for the TMB- H_2O_2 reactions (Fig. S8). Accordingly, no significant change in the catalysis performances of Hem-Au@apoHb composites was observed even though they were stored in water up to six months, thus confirming the high environmental stability.

3.6. Preliminary catalysis applications

The feasibility of practical application of the Hem-Au@apoHb was investigated by the preliminary colorimetric assays for H_2O_2, in comparison to natural Hb. Fig. 3 describes the comparison of colorimetric H_2O_2 results between Hem-Au@apoHb (Fig. 3A) and Hb (Fig. 3B). As can be seen from Fig. 3A, Hem-Au@apoHb could facilitate the detection of H_2O_2 with the concentrations linearly ranging from 0.0050 to 2.20 mM, with a detection limit of about 1.25 μM, estimated by the 3σ rule. In contrast, the colorimetric analysis with natural Hb could allow for the detection of H_2O_2 in the linear concentrations from 0.010 to 1.0 mM, with a detection limit of about 5.0 μM (Fig. 3B). Also, the H_2O_2 detection range of the developed analysis using Hem-Au@apoHb is wider than that of the detection method with Hemin@metal-organic framework elsewhere (0.0050–0.20 mM) (Qin et al., 2013). Moreover, the detection sensitivity of this work was calculated to be 1.23 mM^{-1} (by the calibration curve slope), which is a little higher than that of the one reported previously (0.750 mM^{-1}) (Jv et al., 2010). Moreover, the direct H_2O_2 electroanalysis with the Hem-Au@apoHb-modified electrode was explored by comparing to the Hb-modified electrode, where the signal outputs of linear sweep voltammograms (LSVs) were performed, with the results shown in Fig. 4A. It is noted that the LSV potential of the Hem-Au@apoHb-modified electrode could peak at about −0.30 V, which is lower than that of the Hb-modified one peaking at −0.35 V. Apparently, a more efficient electron-transferring could be expected for the Hem-Au@apoHb-modified electrode. Remarkably, the LSV responses to H_2O_2 of the Hem-Au@apoHb-modified electrode are over four-fold larger than those of the Hb-modified electrode, showing the much higher electrocatalysis for H_2O_2. Moreover, the electrocatalysis performances of the Hem-Au@apoHb electrode were further investigated in sensing H_2O_2 with different concentrations, with the corresponding calibration plots shown in Fig. 4B. It is found that H_2O_2 could be detected in the concentrations ranging from 0.0018 to 2.50 mM, with a detection limit of about 0.45 μM (by 3σ rule) that is comparable to that of the HRP-modified electrode reported elsewhere (0.42 μM) (Xu et al., 2010). In addition, as can be shown from the current-time curve (Fig. 4B, inset), the Hem-Au@apoHb electrode could show the rapid steady-state current responses (within 5 s) which increased stepwise with the successive additions of H_2O_2. Obviously, the Hem-Au@apoHb elec-

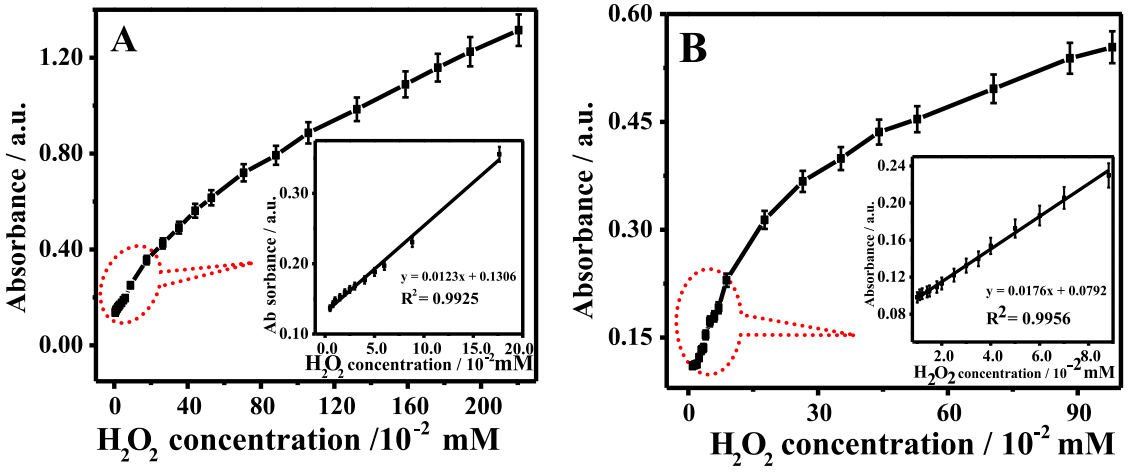

Fig. 3. Comparison of colorimetric H_2O_2 results between (A) Hem-Au@apoHb and (B) Hb each with 2.03 μM Hem by using different concentrations of H_2O_2 from 0.0050 to 2.20 mM.

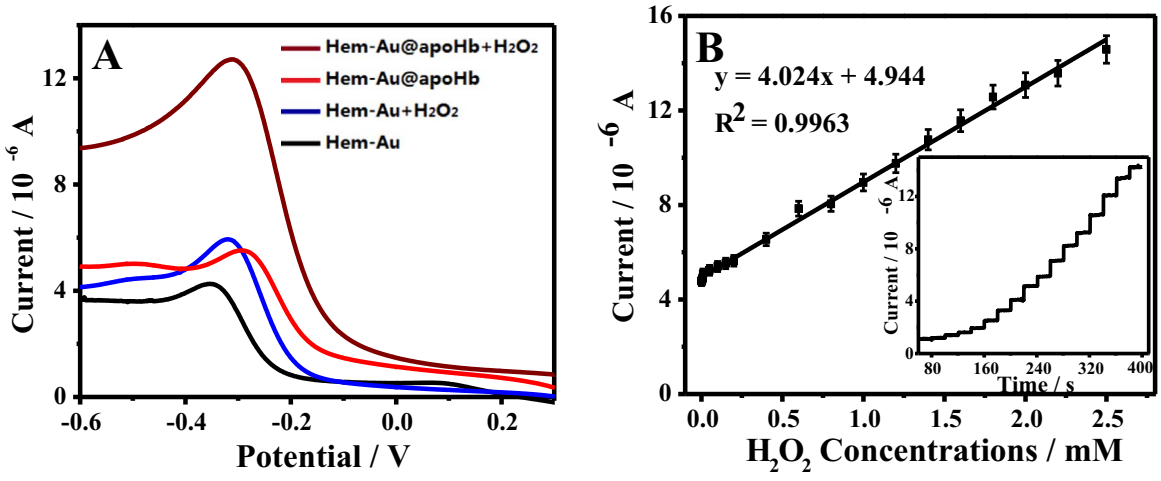

Fig. 4. (A) Comparison of electrochemical responses between the electrodes modified separately with Hem-Au@apoHb and Hb before and after the addition of H_2O_2 (10 μM); (B) the calibration curve of the electrode modified with Hem-Au@apoHb by plotting the current responses versus different H_2O_2 concentrations ranging from 0.0018 to 2.50 mM with the corresponding amperometric responses (insert), which were recorded at the successive additions of H_2O_2 at a step of 10 μM at a potential of −0.30 V.

trode could allow for the direct electroanalysis for H_2O_2 with the fast response and high detection sensitivity. Therefore, the above results indicate that the developed Hem-Au@apoHb-based assays could facilitate the better or comparable performances for the analysis of H_2O_2. Importantly, the reconstituted peroxidase mimics of Hem-Au@apoHb could present additionally some advantages over the traditional catalysis materials like cost-effectiveness, improved catalysis, high environmental stability, and fast electrocatalysis response, thus promising the extensive applications in different catalysis-based detection fields.

4. Conclusions

A novel enzymatic reconstitution methodology has been successfully developed by extracting the redox active centers from Hb for the in-site gold biomineralization to be further reconstituted into apoHb yielding the high-catalysis Hem-Au@apoHb nanocomposites for sensing H_2O_2. As evidenced in the colorimetric assays and direct electroanalysis detections, the obtained peroxidase mimics could present the greatly improved intrinsic catalysis and electrocatalysis activities, which are over four- and 10-fold stronger than those of natural Hb and Hem, respectively. Moreover, steady-state kinetics studies indicate that the developed artificial peroxidases could achieve the higher substrate affinity and intrinsic catalysis capacities than natural Hb and even some peroxidases like HRP, as demonstrated by lower K_m values. Herein, the introduction of the biomineralized gold into Hem scaffolds could not only functionalize as “nanowires” to accelerate the electron transferring, but also create the reactivity pathways for pre-organizing more substrates (i.e., TMB) to the active sites of Hem-Au@apoHb achieving the high substrate affinity. H_2O_2 could be quantified by the Hem-Au@apoHb-based colorimetric and electrocatalytic assays in the linear concentrations ranging from 0.0050 to 2.20 mM and 0.0018 to 2.50 mM, respectively. Although the detailed mechanism should be investigated further, the enzymatic reconstitution methodology with active centers remolded by gold “nanowires” may expand the application scope of heme-containing proteins or enzymes in the various catalysis fields. For example, Hem-Au@apoHb nanocomposites so prepared may be employed to probe the H_2O_2 levels in some other biological samples like cells, which will be conducted in the future work.

Acknowledgments

This work is supported by the National Natural Science Foundation of China (Nos. 21375075 and 21675099) and the Taishan Scholar Foundation of Shandong Province, P.R. China.

Appendix A. Supplementary material

Supplementary data associated with this article can be found in the online version at doi:10.1016/j.bios.2016.09.075.

References

Andersen, C.B.F., Torvund-Jensen, M., Nielsen, M.J., de Oliveira, C.L.P., Hersleth, H.-P., Andersen, N.H., Pedersen, J.S., Andersen, G.R., Moestrup, S.K., 2012. Nature 489 (7416), 456–459.
Boys, B.L., Kuprowski, M.C., Konermann, L., 2007. Biochemistry 46 (37), 10675–10684.
Chen, W., Cai, S., Ren, Q.-Q., Wen, W., Zhao, Y.-D., 2012. Analyst 137 (1), 49–58.
Clouthier, C.M., Pelletier, J.N., 2012. Chem. Soc. Rev. 41 (4), 1585–1605.
Dydio, P., Reek, J.N., 2014. Chem. Sci. 5 (6), 2135–2145.
Erickson, H.P., 2009. Biol. Proced. Online 11 (1), 32.
Gao, L.Z., Zhuang, J., Nie, L., Zhang, J.B., Zhang, Y., Gu, N., Wang, T.H., Feng, J., Yang, D.L., Perrett, S., Yan, X.Y., 2007. Nat. Nanotechnol. 2 (9), 577–583.
Hayashi, T., Hitomi, Y., Ogoshi, H., 1998. J. Am. Chem. Soc. 120 (20), 4910–4915.
Hayashi, T., Hitomi, Y., Ando, T., Mizutani, T., Hisaeda, Y., Kitagawa, S., Ogoshi, H., 1999. J. Am. Chem. Soc. 121 (34), 7747–7750.
Heller, A., 1990. Acc. Chem. Res. 23 (5), 128–134.
Huang, C.C., Bai, H., Li, C., Shi, G.Q., 2011. Chem. Commun. 47 (17), 4962–4964.
Jones, E.M., Balakrishnan, G., Spiro, T.G., 2012. J. Am. Chem. Soc. 134 (7), 3461–3471.
Jv, Y., Li, B., Cao, R., 2010. Chem. Commun. 46 (42), 8017–8019.
Mai, Z.B., Zhao, X.J., Dai, Z., Zou, X.Y., 2010. Talanta 81 (1), 167–175.
McCarthy, M.R., Vandegriff, K.D., Winslow, R.M., 2001. Biophys. Chem. 92 (1), 103–117.
Patolsky, F., Weizmann, Y., Willner, I., 2004. Angew. Chem. Int. Ed. 43 (16), 2113–2117.
Qin, F.-X., Jia, S.-Y., Wang, F.-F., Wu, S.-H., Song, J., Liu, Y., 2013. Catal. Sci. Technol. 3 (10), 2761–2768.
Raynal, M., Ballester, P., Vidal-Ferran, A., van Leeuwen, P.W., 2014a. Chem. Soc. Rev. 43 (5), 1660–1733.
Raynal, M., Ballester, P., Vidal-Ferran, A., van Leeuwen, P.W., 2014b. Chem. Soc. Rev. 43 (5), 1734–1787.
Ryabov, A.D., Goral, V.N., Gorton, L., Csöregi, E., 1999. Chem. Eur. J. 5, 961–967.
Shamsipur, M., Pashabadi, A., Molaabasi, F., 2015. RSC Adv. 5 (76), 61725–61734.
Shan, D., Han, E., Xue, H.G., Cosnier, S., 2007. Biomacromolecules 8 (10), 3041–3046.
Si, Y.M., Sun, Z.Z., Zhang, N., Qi, W., Li, S.Y., Chen, L.J., Wang, H., 2014. Anal. Chem. 86 (20), 10406–10414.
Song, H.-Y., Liu, J.-Z., Weng, L.-P., Ji, L.-N., 2009. J. Mol. Catal. B Enzym. 57 (1), 48–54.
Torres, E., Baeza, A., Vazquez-Duhalt, R., 2002. J. Mol. Catal. B Enzym. 19, 437–441.
Wang, C.L., Astruc, D., 2014. Chem. Soc. Rev. 43 (20), 7188–7216.
Wang, H., Li, S., Si, Y.M., Sun, Z.Z., Li, S.Y., Lin, Y.H., 2014a. J. Mater. Chem. B 2 (28), 4442–4448.
Wang, H., Li, S., Si, Y.M., Zhang, N., Sun, Z.Z., Wu, H., Lin, Y.H., 2014b. Nanoscale 6 (14), 8107–8116.
Wang, Q.-Q., Gonell, S., Leenders, S.H., Dürr, M., Ivanović-Burmazović, I., Reek, J.N., 2016. Nat. Chem..
Wei, H., Wang, E., 2013. Chem. Soc. Rev. 42 (14), 6060–6093.
Willner, I., Heleg-Shabtai, V., Blonder, R., Katz, E., Tao, G., Bückmann, A.F., Heller, A., 1996. J. Am. Chem. Soc. 118 (42), 10321–10322.

Wilson, M.S., Nie, W., 2006. Anal. Chem. 78 (8), 2507–2513.
Xia, P.P., Liu, H.Q., Tian, Y., 2009. Biosens. Bioelectron. 24 (8), 2470–2474.
Xiao, Y., Patolsky, F., Katz, E., Hainfeld, J.F., Willner, I., 2003. Science 299 (5614), 1877–1881.
Xie, J.P., Zheng, Y.G., Ying, J.Y., 2009. J. Am. Chem. Soc. 131 (3), 888–889.
Xie, J.X., Zhang, X.D., Wang, H., Zheng, H.Z., Huang, Y.M., 2012. TrAC Trends Anal. Chem. 39, 114–129.
Xu, J., Shang, F.J., Luong, J.H., Razeeb, K.M., Glennon, J.D., 2010. Biosens. Bioelectron. 25 (6), 1313–1318.
Yang, X., Yang, M.X., Pang, B., Vara, M., Xia, Y.N., 2015. Chem. Rev. 115 (19), 10410–10488.
Yehezkeli, O., Yan, Y.M., Baravik, I., Tel-Vered, R., Willner, I., 2009. Chem. Eur. J. 15 (11), 2674–2679..
Zhang, N., Si, Y.M., Sun, Z.Z., Chen, L.J., Li, R., Qiao, Y.C., Wang, H., 2014. Anal. Chem. 86 (23), 11714–11721.